Organometallics **1994,** *13,* 172-178

Coordinatively Unsaturated Complexes $[Fe_2(CO)_5(\mu\text{-}PBu^t_2)(\mu\text{-}PR_2)]$(*Fe*═*Fe*) (R = Cy, Ph): Addition of PBu^n_3, Ph_2PH, and dppm (dppm = Bis(diphenylphosphino)methane). The Unprecedented Complex $[Fe_2(CO)_3(\mu\text{-}PBu^t_2)(\mu\text{-}PCy_2)(\mu\text{-}dppm)]$(*Fe*—*Fe*)

Bernhard Walther,* Helmut Hartung,* Sergio Bambirra, André Krug, and
Hans-C. Böttcher

*Department of Chemistry, Martin Luther University Halle-Wittenberg,
D-06099 Halle (Saale), Germany*

Received March 9, 1993[•]

A convenient synthesis of the saturated complexes $[Fe_2(CO)_6(\mu\text{-}PBu^t_2)(\mu\text{-}PR_2)]$ (R = Cy (**4**), Ph (**5**)) and their photochemical in situ transformation into the corresponding unsaturated diiron pentacarbonyl complexes **2** and **3** are described. These compounds readily add PBu^n_3 and Ph_2PH, respectively, in the molar ratio 1:1 to give the complexes $[Fe_2(CO)_5(\mu\text{-}PBu^t_2)(\mu\text{-}PR_2)(PR'_2R'')]$ (R = Cy, R′ = R″ = Bu^n (**6**); R′ = Ph, R″ = H (**7**); R = R′ = Ph, R″ = H (**8**)). Complex **6** reacts under UV irradiation with excess PBu^n_3 to afford the complex $[Fe_2(CO)_4(\mu\text{-}PBu^t_2)(\mu\text{-}PCy_2)(PBu^n_3)_2]$ (**9**). Treatment of **2** with dppm (dppm = bis(diphenylphosphino)methane) gives after subsequent photolysis the unprecedented triply-bridged complex $[Fe_2(CO)_3(\mu\text{-}PBu^t_2)(\mu\text{-}PCy_2)(\mu\text{-}dppm)]$ (**10**). Complex **10**, formally belonging to the complexes of general formula $[Fe_2L_5(\mu\text{-}PR_2)_2]$ (L = 2e ligand) with an iron–iron double bond, shows only an iron–iron single bond distance (2.631(1) Å) due to the bent $Fe_2(\mu\text{-}P\langle)_2$ core ($\theta = 107.6°$) caused by the bridging dppm ligand. The molecular structures of complexes **6**, **7**, and **10** are described.

Introduction

Coordinative unsaturation usually (i.e. in the absence of severe steric hindrance) provides a high reactivity for the complexes concerned. The most important type of reaction to illustrate unsaturation is the addition reaction, which requires a sufficient low energy acceptor orbital (LUMO). In metal–metal bonded complexes, one result of coordinative unsaturation is formation of metal–metal multiple bonds. Outstanding examples are $[Mo_2cp_2(CO)_4]$ and $[Os_3(CO)_{10}(\mu\text{-}H)_2]$ considered to have a MoMo triple bond and an OsOs double bond, respectively. Starting with these complexes an extensive organometallic and cluster chemistry has been developed.[1,2]

Recently, we[3] and others[4] described the new electron-poor complex $[Fe_2(CO)_6(\mu\text{-}PBu^t_2)_2]$(*Fe*═*Fe*) (**1**) obtained by different synthetic routes. Furthermore, we reported that two other complexes of this type $[Fe_2(CO)_5(\mu\text{-}PBu^t_2)(\mu\text{-}PR_2)]$ (R = Cy (**2**),[5] Ph (**3**)[3]) can be prepared from the appropriate electron-precise complexes $[Fe_2(CO)_6(\mu\text{-}PBu^t_2)(\mu\text{-}PR_2)]$ (**4**, **5**) by thermal CO dissociation.

Hoffmann[6] has discussed that, from the viewpoint of the isolobal relationship $Fe(CO)_4 \leftarrow\!\circ\!\rightarrow CH_2$, one might expect the unsaturated binuclear carbonyl $[(CO)_4Fe{=}Fe(CO)_4]$ but that, due to the small π/π^* gap, this molecule easily adds CO to give the saturated diiron nonacarbonyl. Complexes $[Fe_2(CO)_5(\mu\text{-}PR_2)_2]$ are isolobal with $[Fe_2(CO)_8]$(*Fe*═*Fe*), and EHMO calculations confirmed that their frontier orbitals are π/π^* in nature.[3] Obviously, for complexes **2** and **3** the π/π^* gap is sufficiently high in energy to make them isolable but leaves from operationally reactive to add ligands except for complex **1**[3,7] where the bulky $\mu\text{-}PBu^t_2$ ligands prevent addition reactions. Such addition reactions are the subject of this paper including the structural characterization of the products obtained.

Experimental Section

General Comments. Reactions were performed under oxygen-free argon using conventional Schlenk techniques. Photochemical reactions were carried out with a Hereaus TQ 150 high pressure mercury lamp in a 250-mL photoreactor equipped with an argon line adapter, stirbar, rubber septum, and an argon delivery tube. Solvents were dried over molecular sieves or over sodium/benzophenone ketyl and distilled under argon prior to use. Starting materials were either commercially available or were prepared according to literature procedures: Bu^t_2PCl,[8] Cy_2PCl,[9] Ph_2PCl,[10] $Na_2[Fe(CO)_4]\cdot 1.5(dioxane)$.[11]

IR spectra were obtained using an IR 71 instrument of VEB Carl Zeiss Jena. ^1H and ^{31}P NMR spectra were recorded on the Bruker spectrometers WP 200 (^1H at 200.13 MHz, ^{31}P at 81.02 MHz) and AC 80 (^1H at 80.13 MHz, ^{31}P at 32.43 MHz). Chemical shift references are the absolute frequencies of Me_4Si (^1H) and external 85% H_3PO_4(aq) (^{31}P), respectively. Positive shifts are to lower field.

[•] Abstract published in *Advance ACS Abstracts,* October 1, 1993.

[1] Curtis, M. D. Polyhedron **1987,** *6,* 759 and references given therein.

[2] Lavigne, G. In *The Chemistry of Metal Cluster Compounds*; Shriver, D. F., Kaesz, H. D., Adams, R. D., Eds.; VCH: New York, 1990; Chapter 5, pp 201–302.

[3] Walther, B.; Hartung, H.; Reinhold, J.; Jones, P. G.; Mealli, C.; Böttcher, H.-C.; Baumeister, U.; Krug, A.; Möckel, A. *Organometallics* **1992,** *11,* 1542 and references given therein.

[4] Adams, M. R.; Galluci, J.; Wojcicki, A. *Inorg. Chem.* **1991,** *31,* 2.

[5] Walther, B.; Hartung, H.; Reinhold, J.; Jones, P. G.; Böttcher, H.-C.; Baumeister, U.; Krug, A. *Chem. Ber.* **1992,** *125,* 1379.

[6] Hoffmann, R. *Angew. Chem., Int. Ed. Engl.* **1982,** *21,* 711.

[7] Knoll, H.; Hennig, H.; Walther, B.; Böttcher, H.-C.; Stufkens, D. J. *Inorg. Chim. Acta* **1993,** *210,* 33.

[8] Field, M.; Stelzer, O.; Schmutzler, R. *Inorg. Synth* **1973,** *14,* 4.

[9] Issleib, K.; Seidel, W. *Chem. Ber.* **1959,** *92,* 2681.

[10] Brown, M. P.; Silver, H. B. *Chem. Ind.* **1991,** 24.

[11] Finke, R. G.; Sorrell, T. N. *Org. Synth.* **1980,** *59,* 102.

0276-7333/94/2313-0172$04.50/0

Table I. Summary of Crystallographic Data for Compounds 6, 7, and 10-CH_2Cl_2

	6	7	10-CH_2Cl_2
empirical formula	$C_{37}H_{67}O_5P_3Fe_2$	$C_{37}H_{51}O_5P_3Fe_2$	$C_{49}H_{64}O_3P_4Cl_2Fe_2$
mw	796.6	780.4	1007.5
cryst syst	monoclinic	monoclinic	monoclinic
space group	*Cc*	$P2_1/n$	*Cc*
lattice constants			
a (Å)	25.772(5)	17.184(4)	21.930(3)
b (Å)	11.891(3)	26.641(3)	12.845(1)
c (Å)	19.583(4)	17.756(4)	18.153(2)
β (°)	135.385(8)	105.88(1)	103.345(8)
V ($Å^3$)	4215(2)	7819(3)	4975.5(10)
Z	4	8	4
F(000)	1704	3280	2112
D_{calc} (g cm^{-1})	1.255	1.326	1.345
μ(Mo Kα) (cm^{-1})	8.4	9.0	8.6
cryst dimens (mm)	0.59 × 0.44 × 0.49	0.40 × 0.37 × 0.36	0.38 × 0.46 × 0.42
diffractometer	Stoe Stadi4	Stoe Stadi4	Stoe Stadi4
temp (K)	293	293	293
check reflns	020, 004, $\bar{3}\bar{1}0$	230, $0\bar{4}0$, $\bar{4}0\bar{2}$	006, $\bar{4}00$, $8\bar{2}0$
intensity variation (%)	±3.5, ±4.4, ±3.7	±3.5, ±4.2, ±3.6	±3.6, ±3.6, ±3.8
no. of unique reflns	3558	11255	8597
range of measmnt (deg)	$3 \leq 2\theta \leq 50$	$3 \leq 2\theta \leq 51$	$3 \leq 2\theta \leq 50$
min *h*,*k*,*l*/max *h*,*k*,*l* (set 1)	−20,0,−23/30,14,0	−20,0,0/20,32,21	−26,0,0/25,15,21
min *h*,*k*,*l*/max *h*,*k*,*l* (set 2)		−15,−2,−17/16,0,0	−25,−15,−21/26,0,0
no. of reflns obsd	3065 ($I \geq 2.00\sigma(I)$)	4747 ($I \geq 2.00\sigma(I)$)	7962 ($I \geq 1.96\sigma(I)$)
reflns/param	7.4	5.6	14.8
weighting scheme	$w = 1.72/(\sigma^2(F_o) + 0.0005F_o^2)$	$w = 2.04/(\sigma^2(F_o) + 0.0002F_o^2)$	$w = 0.90/(\sigma^2(F_o) + 0.0004F_o^2)$
max shift/σ (last least squares cycle)	0.037	0.005	0.007
max/min $\Delta\rho$ in diff map (e $Å^{-3}$)	0.65/−0.40	0.48/−0.50	0.53/−0.38
$R(R_w)$	0.047 (0.058)	0.064 (0.046)	0.029 (0.035)
goodness of fit (*S*)	2.29	1.38	1.26

One-Pot Preparation of $[Fe_2(CO)_6(\mu\text{-}PBu^t_2)(\mu\text{-}PR_2)]$ (R = Cy (4), Ph (5)). The photoreactor was charged with a suspension of 4.15 g (12 mmol) of $Na_2[Fe(CO)_4]\cdot1.5$(dioxane) in 250 mL of THF. An equimolar amount of Bu^t_2PCl (2.17 g, 2.18 mL) was added by syringe, and the mixture was stirred for 2 h. Subsequently, 2.35 g (1.61 mL, 12 mmol) of $[Fe(CO)_5]$ was added by syringe. After stirring for 24 h, the reaction mixture was photolyzed until gas evolution was finished (ca. 4 h). The solution of $Na[Fe_2(\mu\text{-}CO)(CO)_6(\mu\text{-}PBu^t_2)]$ obtained was treated with equimolar amounts of R_2PCl (R = Cy, 2.79 g, 2.54 mL; R = Ph, 2.65 g, 2.16 mL) and stirred for 12 h. The reaction mixture was then transferred to a Schlenk tube containing ca. 30 g of silica gel (Merck 60), and the solvent was removed in vacuo. The residue was subjected to column chromatography (Merck 60, 3 × 35 cm, water-cooled, hexane/benzene 5/1, v/v). Elution gave in the case of R = Cy a minor yellow band of $[Fe_2(CO)_6(\mu\text{-}PCy_2)_2]$ followed by a broad deep violet band of 4, yield 5.1 g (68%), mp 190–195 °C dec (pentane). In the case of R = Ph, a minor green band of $[Fe_2(CO)_5(\mu\text{-}PBu^t_2)_2]$ (1) was followed by the deep brown band of 5, yield 3.5 g (48.7%), mp 165–170 °C dec (diethyl ether). Generally, the elution of these diiron hexa(penta)carbonyl complexes under the conditions given decreases as follows: $[Fe_2(CO)_6(\mu\text{-}PCy_2)_2] > 4 > 1 > 5 > [Fe_2(CO)_6(\mu\text{-}PPh_2)_2]$.

Photochemical Standard in Situ Preparation of $[Fe_2(CO)_5(\mu\text{-}PBu^t_2)(\mu\text{-}PR_2)]$ (R = Cy (2), Ph (3)). The photoreactor was charged with 1.24 g or 1.22 g (2 mmol) of compounds 4 or 5, and ca. 250 mL of heptane or THF was added by syringe. The solution was subsequently photolyzed for ca. 90 min while a slow stream of argon was continuously bubbled through it. During this time a color change from violet (4 → 2) or red-brown (5 → 3) to green occurred. The formation of complexes 2 and 3 is quantitative, and their solutions then were utilized in situ. The complexes can, however, also be isolated by evaporation of the solvent in vacuo and workup of the residue as described.[3,5]

Synthesis of $[Fe_2(CO)_5(\mu\text{-}PBu^t_2)(\mu\text{-}PR_2)(PR'_2R'')]$ (R = Cy, R′ = R″ = Bu^n (6); R′ = Ph, R″ = H (7); R = R′ = Ph, R″ = H (8)). The general procedure used was as follows. To the standard solution of 2 and 3, respectively, prepared as described above, was added an equimolar amount of the phosphane (0.41 g of PBu^n_3, 0.37 g of Ph_2PH) by syringe. A rapid color change from green to violet (2 → 6, 7) and red-brown (3 → 8), respectively, occurred. The mixtures were stirred for 30 min, and the volume of the heptane solution was subsequently reduced by evaporation in vacuo until ca. 50 mL remained Compounds 6–8 crystallized at −30 °C and were recrystallized from diethyl ether (6, 8) or heptane (7).

6: 0.81 g, 51%; mp 166–169 °C dec. Anal. Calcd for $C_{37}H_{67}Fe_2O_5P_3$: C, 55.77; H, 8.41; P, 11.68. Found: 55.40; H, 8.57; P, 11.53. IR, terminal carbonyl region (hexane): 1994 (s), 1941 (s), 1921 (sh), 1913 (vs), 1873 (s) cm^{-1}.

7: 0.62 g, 79%; mp 136–140 °C dec. Anal. Calcd for $C_{37}H_{51}Fe_2O_5P_3$: C, 56.90; H, 6.50; P, 11.92. Found: 57.11; H, 6.82; P, 11.59. IR, terminal carbonyl region (hexane): 1989 (s), 1927 (m), 1920 (sh), 1911 (vs), 1874 (s) cm^{-1}. ^1H NMR (C_6D_6): δ 1.29 (d, ^3J(PH) = 132 Hz, PBu^t_2), 3.0–1.5 (m, PCy_2), 7.2 (d, ^1J(PH) = 356.9 Hz, Ph_2PH).

8: 0.53 g, 68%; mp 150–155 °C dec. Anal. Calcd for $C_{37}H_{39}Fe_2O_5P_3$: C, 57.80; H, 5.07; P, 12.10. Found: C, 57.43; H, 4.99; P, 11.92. IR, terminal carbonyl region (hexane): 2014 (s), 2003 (m), 1959 (s), 1956 (vs), 1930 (w), 1908 (m) cm^{-1}.

Reaction of Complex 6 with PBu^n_3. The photoreactor was charged with 0.55 g (0.7 mmol) of complex 6, 0.28 g (1.4 mmol) of PBu^n_3, and 250 mL of THF, and the mixture was irradiated for 90 min. During this time rapid CO evolution occurred. The solvent was then removed in vacuo and the oily residue was kept at 10^{-3} Torr for 2 h to remove excess PBu^n_3. No crystallization could be achieved but ^{31}P NMR spectroscopy (Table V) unequivocally proved the presence of the disubstituted complex $[Fe_2(CO)_4(\mu\text{-}PBu^t_2)(\mu\text{-}PCy_2)(PBu^n_3)_2]$ (9).

Reaction of Complex 2 with dppm. To a solution of 2, prepared as described above from 0.62 g (1 mmol) of 4 in 240 mL of THF, was added 0.38 g (1 mmol) of dppm in 10 mL of THF. The green color of 2 was discharged to produce a violet-brown solution. The solution was stirred for 2 h and then photolyzed for an additional 2 h while argon was bubbled through the mixture. The THF was removed in vacuo. Recrystallization from ca. 10 mL petroleum ether at −30 °C gave 0.79 g (83%) of 10, mp 150–154 °C dec. Anal. Calcd for $C_{48}H_{62}Fe_2O_3P_4$: C, 62.48; H, 6.77; P, 13.43. Found: C, 62.31; H, 6.35; P, 13.12. IR, terminal carbonyl region (Nujol): 1912 (vs), 1878 (vs), 1853 (s) cm^{-1}.

X-ray Crystallography. A summary of crystal data and details of the structure determinations are given in Table I. All measurements were performed using graphite-monochromated

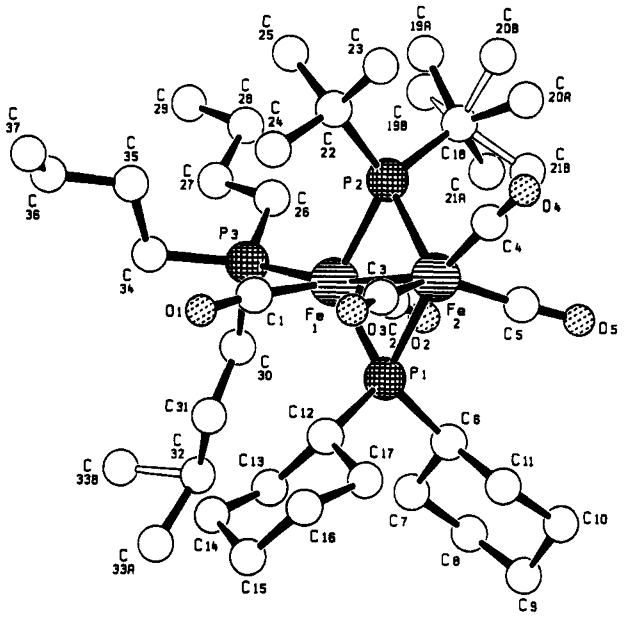

Figure 1. Molecular structure of $[Fe_2(CO)_5(\mu\text{-}PBu^t_2)(\mu\text{-}PCy_2)(PBu^n_3)]$ (6) with atom labels.

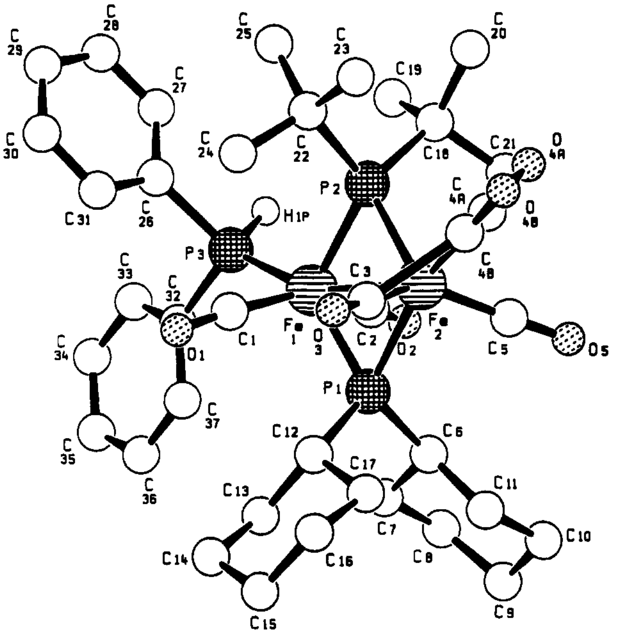

Figure 2. Molecular structure of $[Fe_2(CO)_5(\mu\text{-}PBu^t_2)(\mu\text{-}PCy_2)(PHPh_2)]$ (7, molecule I) with atom labels.

Mo Kα radiation on a Stoe four-circle diffractometer Stadi4 in the ω/θ scanning mode at room temperature. Lattice constants were obtained by a least-squares treatment of the setting angles of 76, 84, and 80 reflections for 6, 7, and 10·CH_2Cl_2, respectively. Lorentz and polarization corrections were applied during data reduction. For all three compounds empirical absorption corrections based on ψ-scan measurements were performed (relative transmission factors between 0.638 and 0.743 for 6, between 0.712 and 0.776 for 7, between 0.742 and 0.789 for 10·CH_2Cl_2). The structures of 6 and 10·CH_2Cl_2 were solved by the Patterson method (SHELXS-86[12]); that of 7 was solved by direct methods (SHELXS-86[12]). Full-matrix least-squares refinement on F including all non-H atoms gives anomalously high U_{iso} values for the terminal C atoms of Bu^n and Bu^t groups in 6 and for one CO ligand in molecule I of 7 as well as unsatisfactory bond lengths and angles for the above mentioned moieties. Both effects point to disorder phenomena. Consequently in difference Fourier maps two alternative positions A and B for the three terminal C atoms of one Bu^t group and the terminal C atom of one Bu^n group in 6 and for one CO ligand in 7 could be indicated. The described positional disorder was taken into consideration by relative site occupation factors for the atoms in question refined in all cases to approximately 0.5. The disordered atoms (labeled in Figures 1 and 2 with A and B, respectively) were refined isotropically with a group displacement parameter assigned to the Bu^t group and individual ones for the three other atoms. All other non-H atoms of the three compounds were subjected to an anisotropic refinement. For 7 each of the two independent molecules was refined in a separate block. For 10·CH_2Cl_2, in a difference Fourier map three additional peaks of considerable height (3–12 e Å^{-3}) were found which pointed to the presence of dichloromethane (constituent of the solvent mixture used for recrystallization of 10). The subsequent refinement as well as density measurements confirmed that the ratio of complex 10 to CH_2Cl_2 equals 1:1 in the crystal lattice. The solvent molecule and the phenyl rings in 10 were also refined in a separate block. The two H atoms linked to the P atoms of the diphenylphosphine ligand in 7 were located in a difference map and refined individually. All other H atoms positioned by geometric calculations were included using the riding model according to SHELX-76.[13] The absolute structure of 6 was determined by Flack's x refinement[14] (the parameter x amounts to −0.04(3) for the specified atomic coordinate set); that of 10, by comparison of R values of the two structures being inverse to each other (0.029 and 0.044, respectively). Final non-H atomic parameters are summarized in Tables II–IV.

Results and Discussion

Reaction of $[Fe_2(CO)_5(\mu\text{-}PBu^t_2)(\mu\text{-}PR_2)]$ (2, 3) with PR'_2R'' ($R' = Bu^n, Ph, R'' = Bu^n, H$). In previous papers we described the preparation of the electron-poor complexes $[Fe_2(CO)_5(\mu\text{-}PBu^t_2)(\mu\text{-}PR_2)]$ (R = Cy (2), Ph (3)) from the electron-precise diiron hexacarbonyl complexes 4 and 5 either by thermal CO dissociation[5,3] or by irradiation with the 457.9-nm line of an argon laser.[7]

This paper shows that (i) solutions of these complexes can most conveniently be obtained by photolysis of compounds 4 and 5 in THF or n-heptane with a high pressure mercury lamp if the eliminated carbon monoxide is removed by bubbling argon through the solution, and (ii) the starting diiron hexacarbonyl complexes can be prepared by a one-pot synthesis on a scale of up to 3–5 g (see Experimental Section).

We have recently shown that the electron-poor complex $[Fe_2(CO)_5(\mu\text{-}PBu^t_2)_2]$ (1) does not exhibit any tendency to add neutral ligands like CO[3] or PR_3 (R = Bu^n, OMe),[7] and have explained this failure with the particular bulkiness of the bridging ligands involved.

Complexes 2 and 3 behave quite differently compared with 1. E.g. they do exist in equilibrium with their electron-precise counterparts 4 and 5 according to eq 1 and their

$$4,5 \underset{+CO}{\overset{-CO}{\rightleftharpoons}} 2,3 \qquad (1)$$

isolation requires the removal of CO from the equilibrium. The $Fe_2(\mu\text{-}P)_2$ core geometry of complex 4 is exactly planar (θ = 180°, this mirror plane also includes two carbonyl ligands[5]), and that of 2 and 3 is nearly planar (θ = 169°,[5]

---

[12] Sheldrick, G. M. SHELXS-86, Program for crystal structure determination, University of Göttingen, FRG, 1986.

[13] Sheldrick, G. M. SHELX-76, Program for crystal structure determination, University of Cambridge, England, 1976.

[14] Flack, H. D. *Acta Crystallogr.* **1983**, *A39*, 876.

Table II. Fractional Coordinates and Equivalent Isotropic Displacement Parameters (Å^2) for the Non-Hydrogen Atoms of 6

atom	x/a	y/b	z/c	U_{eq}[a]
Fe1	–0.07295(7)	–0.66065(8)	–0.04917(9)	0.0433(7)
Fe2	0.00000	–0.85709(8)	0.00000	0.0508(9)
P1	–0.0748(1)	–0.8092(2)	0.0185(2)	0.045(1)
P2	–0.0046(1)	–0.7077(2)	–0.0766(2)	0.050(1)
P3	–0.1208(1)	–0.4863(2)	–0.0951(2)	0.058(1)
O1	0.0273(3)	–0.5551(5)	0.1436(4)	0.072(4)
O2	–0.2230(3)	–0.7181(6)	–0.2302(4)	0.087(5)
O3	0.1256(4)	–0.8443(7)	0.2106(5)	0.091(5)
O4	0.1017(5)	–0.9899(7)	0.0147(7)	0.111(8)
O5	–0.1070(5)	–1.0287(8)	–0.1403(8)	0.127(9)
C1	–0.0088(4)	–0.5984(6)	0.0676(6)	0.053(6)
C2	–0.1623(5)	–0.7000(7)	–0.1604(6)	0.061(7)
C3	0.0760(5)	–0.8437(7)	0.1290(7)	0.064(7)
C4	0.0614(6)	–0.9348(8)	0.0067(7)	0.073(8)
C5	–0.0689(6)	–0.9568(9)	–0.0880(8)	0.084(10)
C6	–0.1626(5)	–0.8924(7)	–0.0528(6)	0.056(6)
C7	–0.2214(5)	–0.8361(8)	–0.0668(7)	0.074(7)
C8	–0.2934(5)	–0.9025(10)	–0.1371(7)	0.083(7)
C9	–0.2833(6)	–1.0214(11)	–0.1063(9)	0.104(9)
C10	–0.2215(6)	–1.0804(9)	–0.0901(9)	0.099(10)
C11	–0.1498(6)	–1.0143(7)	–0.0165(8)	0.079(8)
C12	–0.0295(4)	–0.7970(6)	0.1458(5)	0.047(5)
C13	–0.0728(5)	–0.7256(7)	0.1580(6)	0.065(7)
C14	–0.0206(5)	–0.6965(8)	0.2649(6)	0.076(7)
C15	0.0128(6)	–0.8043(10)	0.3302(7)	0.090(9)
C16	0.0507(6)	–0.8755(8)	0.3133(6)	0.078(7)
C17	–0.0034(5)	–0.9064(7)	0.2030(6)	0.064(7)
C18	–0.0490(5)	–0.7396(7)	–0.2050(6)	0.068(7)
C19A	–0.0464(12)	–0.6384(13)	–0.2525(15)	0.080(2)[b]
C19B	–0.0904(12)	–0.6371(13)	–0.2713(13)	0.080(2)[b]
C20A	–0.0150(11)	–0.8429(13)	–0.2075(15)	0.080(2)[b]
C20B	0.0020(10)	–0.7792(18)	–0.2162(15)	0.080(2)[b]
C21A	–0.1331(6)	–0.7590(18)	–0.2737(12)	0.080(2)[b]
C21B	–0.1010(10)	–0.8418(13)	–0.2488(14)	0.080(2)[b]
C22	0.0873(4)	–0.6367(6)	–0.0097(5)	0.060(6)
C23	0.1433(7)	–0.7112(10)	0.0040(11)	0.12(1)
C24	0.1267(5)	–0.6066(8)	0.0945(5)	0.075(6)
C25	0.0772(6)	–0.5247(9)	–0.0570(8)	0.109(9)
C26	–0.1641(5)	–0.4432(6)	–0.2140(6)	0.073(7)
C27	–0.1959(7)	–0.3248(7)	–0.2488(7)	0.092(9)
C28	–0.2320(8)	–0.3028(10)	–0.3522(8)	0.12(1)
C29	–0.2593(10)	–0.1817(10)	–0.3851(12)	0.15(2)
C30	–0.2103(8)	–0.4767(13)	–0.1240(10)	0.13(1)
C31	–0.1995(9)	–0.4947(16)	–0.0388(12)	0.16(2)
C32	–0.2728(9)	–0.4722(20)	–0.0710(15)	0.19(2)
C33A	–0.2660(22)	–0.4655(40)	0.0127(23)	0.19(2)[b]
C33B	–0.2765(29)	–0.3477(23)	–0.0552(45)	0.23(3)[b]
C34	–0.0752(7)	–0.3640(10)	–0.0136(10)	0.13(1)
C35	–0.0073(7)	–0.3282(10)	0.0120(11)	0.15(2)
C36	0.0339(10)	–0.2266(14)	0.0819(17)	0.21(2)
C37	0.1159(12)	–0.2372(24)	0.1700(18)	0.40(6)

[a] $U_{eq} = {}^1/_3\sum_i\sum_j U_{ij}a^*_i a^*_j \mathbf{a}_i \cdot \mathbf{a}_j$. [b] Isotropic displacement parameters.

166°[3]). Complex 5 on the other hand is butterfly-shaped (θ = 117°[3]), and thus the reaction 5 → 3 involves a flattening of the core geometry. The energy barrier for this process is apparently low enough to be brought about by the π bonding system of complex 3.

Equilibrium 1 promoted us to investigate addition reactions of complexes 2 and 3 with phosphanes PR_3. In the molecular-orbital parlance, nucleophilic addition reactions of these complexes mean the interaction of the HOMO of the entering molecule with the π^*-LUMO of complexes 2 and 3.[3] It is to be expected that the basic structure of the products of the nucleophilic additions is controlled by the steric requirements of the substituents on the μ-PR_2 ligand and is basically the same as for the electron-precise parent complexes 4 and 5 discussed above from which the complexes obtained may be thought of as derived by substitution of one carbonyl ligand for PR_3.

The green complexes 2 and 3, prepared by photolysis in heptane, immediately add equimolar amounts of PBu^n_3 or Ph_2PH according to eq 2 to give violet solutions from

$$[Fe_2(CO)_5(\mu\text{-}PBu^t_2)(\mu\text{-}PR_2)] + PR'_2R'' \rightarrow [Fe_2(CO)_5(\mu\text{-}PBu^t_2)(\mu\text{-}PR_2)(PR_2'R'')] \quad (2)$$

6–8

	6	7	8
R	Cy	Cy	Ph
R′	Bu^n	Ph	Ph
R″	Bu^n	H	H

which complexes [$Fe_2(CO)_5(\mu\text{-}PBu^t_2)(\mu\text{-}PR_2)(PR'_2R'')$] (6–8) can be isolated in good yields. Considering complexes 6–8 formally as substitution products of the saturated complexes 4 and 5, it is worth mentioning that thermal[15,16] and photolytic[17,18] substitution reactions of [$Fe_2(CO)_6(\mu\text{-}PR_2)_2$] with PR_3 were described in the literature to give the mono- and disubstituted products in poor to modest yields. First order rate constants for the thermal substitution reaction of [$Fe_2(CO)_6(\mu\text{-}PPh_2)_2$] with PR_3 (R = Ph, OPh, Bu^n) to give the monosubstituted products have been determined, the rate-limiting step being the dissociative loss of one carbonyl ligand to give [$Fe_2(CO)_5(\mu\text{-}PPh_2)_2$] as a reactive intermediate which is then rapidly trapped by the entering ligand (S_N1 or D mechanism).[15] Compound 6 reacts in THF solution with excess PBu^n_3 under UV irradiation to afford the disubstituted complex [$Fe_2(CO)_4(\mu\text{-}PBu^t_2)(\mu\text{-}PCy_2)(PBu^n_3)_2$] (9) which could not be isolated in crystalline form but was unambiguously identified by phosphorus-31 NMR.

Complexes 6–8 were characterized by elemental analysis and by IR and $^{31}P\{^1H\}$ NMR spectroscopy. The parent complex 4 of compounds 6 and 7 shows only three carbonyl bands due to its high symmetry (1994) cm^{-1}, ν(Fe–(CO)), CO ligand within the mirror plane; 1954 cm^{-1}, ν_s(Fe–(CO)$_2$); 1936 cm^{-1}, ν_{as}(Fe–(CO)$_2$)[5,19]). Substitution of one of the two in-plane carbonyl ligands lowers the symmetry from approximately C_{2v} for 4 to approximately C_s for 6 and 7 (see solid state structure below). Thus, one ν(Fe–(CO)) and both ν_{as}/s(Fe–(CO)$_2$) bands have to be expected, as found in the experimental spectra (see Experimental Section). The frequency of the ν(Fe–(CO)) remains practically constant for compounds 4, 6, and 7. That means that substitution of one of the CO ligands within the mirror plane does not essentially influence the remaining carbonyl ligand. The assignment of the bands of complex 8 and its parent 5 is more questionable. Whereas 5 shows five terminal carbonyl bands, 8 shows six with a shift of the band at the highest wavenumber from 2044 to 2014 cm^{-1}. Obviously, the phosphane ligand exerts a strong influence on the molecule in these butterfly shaped complexes compared to the nearly planar complexes 6 and 7.

The $^{31}P\{^1H\}$ NMR data of compounds 6–9 are summarized in Table V. The NMR spectrum of the disubstituted complex 9 contains besides the signals of a small impurity of 6, two double triplets for the bridging phosphorus nuclei and one double doublet for the equivalent terminal ligands.

---

(15) Gerlach, J. N.; McMullin, S. L.; Ellgen, P. C. *Inorg. Chem.* **1976**, *15*, 1232.

(16) Breen, M. J.; Geoffroy, G. L. *Organometallics* **1982**, *1*, 1437.

(17) Thompson, D. T. *J. Organomet. Chem.* **1965**, *4*, 74.

(18) Collmann, J. P.; Rothrock, B. K.; Finke, R. G.; Moore, E. J.; Rose-Munch, F. *Inorg. Chem.* **1982**, *21*, 146.

(19) U. Kolvenbach, Diploma thesis, Martin Luther University Halle-Wittenberg, 1991.

Table III. Fractional Coordinates and Equivalent Isotropic Displacement Parameters (Å^2) for the Non-Hydrogen Atoms of 7

atom	x/a	y/b	z/c	U_{eq}[a]	atom	x/a	y/b	z/c	U_{eq}[a]
(a) Molecule I									
Fe1	0.72309(6)	0.20773(4)	0.29146(6)	0.0345(5)	C14	0.9258(5)	0.1305(4)	0.5660(5)	0.075(5)
Fe2	0.83178(8)	0.17146(5)	0.22184(8)	0.0567(6)	C15	0.9956(6)	0.0968(4)	0.5609(5)	0.079(5)
P1	0.79757(12)	0.13849(8)	0.32662(13)	0.0390(9)	C16	1.0206(5)	0.1045(4)	0.4868(6)	0.067(5)
P2	0.75152(13)	0.23902(9)	0.18615(12)	0.0448(9)	C17	0.9486(4)	0.0981(3)	0.4145(5)	0.053(4)
P3	0.62814(12)	0.25598(9)	0.31260(12)	0.0388(9)	C18	0.6720(6)	0.2354(4)	0.0861(5)	0.067(4)
O1	0.8325(3)	0.2516(2)	0.4323(3)	0.065(3)	C19	0.5929(5)	0.2603(4)	0.0909(5)	0.082(5)
O2	0.5822(3)	0.1448(2)	0.2247(4)	0.068(3)	C20	0.6993(7)	0.2577(4)	0.0174(5)	0.105(6)
O3	0.9868(4)	0.2052(3)	0.3246(6)	0.136(5)	C21	0.6508(6)	0.1803(4)	0.0640(5)	0.090(5)
O4A	0.8689(9)	0.1873(5)	0.0713(8)	0.067(6)[b]	C22	0.8042(5)	0.3028(3)	0.1900(6)	0.061(4)
O4B	0.9283(10)	0.1890(5)	0.1143(9)	0.081(6)[b]	C23	0.8665(5)	0.3029(3)	0.1417(5)	0.068(4)
O5	0.7704(5)	0.0784(3)	0.1401(4)	0.111(4)	C24	0.8506(5)	0.3139(3)	0.2750(5)	0.063(4)
C1	0.7912(5)	0.2359(3)	0.3753(5)	0.041(4)	C25	0.7431(6)	0.3459(3)	0.1628(6)	0.080(5)
C2	0.6383(5)	0.1690(3)	0.2492(5)	0.045(4)	C26	0.6382(5)	0.3245(3)	0.3232(5)	0.036(3)
C3	0.9250(6)	0.1921(4)	0.2855(7)	0.088(6)	C27	0.5839(5)	0.3550(4)	0.2705(5)	0.050(4)
C4A	0.8510(12)	0.1806(7)	0.1296(14)	0.049(6)[b]	C28	0.5882(6)	0.4061(4)	0.2772(6)	0.069(5)
C4B	0.8952(17)	0.1824(9)	0.1652(14)	0.079(8)[b]	C29	0.6477(7)	0.4279(4)	0.3357(6)	0.067(5)
C5	0.7919(7)	0.1155(4)	0.1736(6)	0.079(6)	C30	0.7016(6)	0.3981(4)	0.3877(6)	0.059(4)
C6	0.7412(4)	0.0781(3)	0.3143(5)	0.042(3)	C31	0.6978(5)	0.3464(3)	0.3826(5)	0.048(4)
C7	0.6847(5)	0.0719(3)	0.3676(5)	0.049(4)	C32	0.5877(4)	0.2396(3)	0.3944(4)	0.038(3)
C8	0.6260(5)	0.0292(3)	0.3375(5)	0.058(4)	C33	0.5197(5)	0.2651(4)	0.4043(5)	0.064(4)
C9	0.6696(5)	−0.0197(3)	0.3318(6)	0.067(4)	C34	0.4894(6)	0.2530(4)	0.4670(6)	0.086(6)
C10	0.7301(5)	−0.0133(3)	0.2834(5)	0.062(4)	C35	0.5257(6)	0.2160(4)	0.5177(6)	0.072(5)
C11	0.7893(5)	0.0297(3)	0.3150(5)	0.048(4)	C36	0.5901(5)	0.1899(4)	0.5079(5)	0.060(4)
C12	0.8810(4)	0.1347(3)	0.4184(4)	0.045(4)	C37	0.6205(5)	0.2012(3)	0.4454(5)	0.048(4)
C13	0.8536(5)	0.1249(4)	0.4930(5)	0.060(4)					
(b) Molecule II									
Fe1	0.29789(6)	0.03034(4)	0.20814(7)	0.0374(5)	C15	0.0200(5)	−0.0983(4)	−0.0143(6)	0.083(5)
Fe2	0.21535(8)	−0.00814(5)	0.30532(7)	0.0501(6)	C16	0.0071(5)	−0.0932(4)	0.0656(6)	0.073(5)
P1	0.23719(13)	−0.04426(8)	0.19675(13)	0.0413(9)	C17	0.0874(5)	−0.0962(3)	0.1291(5)	0.057(4)
P2	0.27713(13)	0.06721(8)	0.31332(13)	0.0422(9)	C18	0.3673(6)	0.0777(4)	0.4017(5)	0.069(5)
P3	0.37118(13)	0.08376(9)	0.16247(14)	0.0448(10)	C19	0.4305(6)	0.1105(4)	0.3793(6)	0.096(5)
O1	0.1725(4)	0.0576(2)	0.0669(4)	0.066(3)	C20	0.3461(6)	0.1013(4)	0.4735(5)	0.090(5)
O2	0.4533(4)	−0.0214(2)	0.2582(4)	0.089(3)	C21	0.4064(6)	0.0277(4)	0.4318(5)	0.098(5)
O3	0.0431(4)	0.0047(3)	0.2260(5)	0.102(4)	C22	0.2060(5)	0.1237(3)	0.3050(6)	0.054(4)
O4	0.1720(5)	0.0060(3)	0.4513(4)	0.108(4)	C23	0.1559(5)	0.1205(3)	0.3642(5)	0.071(5)
O5	0.3116(7)	−0.0877(3)	0.3979(5)	0.157(6)	C24	0.1470(5)	0.1238(3)	0.2234(5)	0.064(4)
C1	0.2194(5)	0.0483(3)	0.1253(5)	0.047(4)	C25	0.2510(5)	0.1741(3)	0.3149(5)	0.074(5)
C2	0.3917(5)	−0.0012(3)	0.2424(5)	0.054(4)	C26	0.3447(5)	0.1504(3)	0.1499(5)	0.047(4)
C3	0.1109(7)	0.0012(4)	0.2541(6)	0.068(5)	C27	0.3947(5)	0.1872(4)	0.1928(6)	0.070(5)
C4	0.1890(6)	0.0024(4)	0.3924(6)	0.073(5)	C28	0.3718(6)	0.2369(4)	0.1822(7)	0.076(5)
C5	0.2768(8)	−0.0558(4)	0.3585(6)	0.088(6)	C29	0.3026(7)	0.2512(4)	0.1284(7)	0.076(6)
C6	0.3032(5)	−0.1007(3)	0.2127(4)	0.040(3)	C30	0.2531(6)	0.2150(4)	0.0857(6)	0.069(5)
C7	0.3453(5)	−0.11114(3)	0.1476(5)	0.049(4)	C31	0.2731(6)	0.1647(3)	0.0950(5)	0.053(4)
C8	0.4119(5)	−0.1504(3)	0.1765(5)	0.056(4)	C32	0.3909(5)	0.0682(4)	0.0699(5)	0.048(4)
C9	0.3798(5)	−0.1984(3)	0.2023(5)	0.060(4)	C33	0.4306(5)	0.1014(4)	0.0340(6)	0.075(5)
C10	0.3325(6)	−0.1885(3)	0.2612(5)	0.068(4)	C34	0.4469(7)	0.0906(5)	−0.0361(7)	0.102(7)
C11	0.2658(5)	−0.1501(3)	0.2312(5)	0.060(4)	C35	0.4247(6)	0.0454(5)	−0.0710(6)	0.090(6)
C12	0.1460(4)	−0.0560(3)	0.1143(4)	0.045(3)	C36	0.3840(6)	0.0119(4)	−0.0372(6)	0.073(5)
C13	0.1613(5)	−0.0650(3)	0.0338(5)	0.055(4)	C37	0.3680(5)	0.0226(4)	0.0329(6)	0.057(4)
C14	0.0814(5)	−0.0613(4)	−0.0306(5)	0.072(5)					

[a] See footnote *a* in Table II. [b] See footnote *b* in Table II.

The Δδ values are roughly twice as great as for compound 6, and the P^{1}P^3 coupling has increased to a value of 8.9 Hz. This spectrum is in full agreement with a structure derived from that of the parent complex 4 by replacement of both in-plane carbonyl ligands by two PBu$^n_3$ ligands.

Molecular Structures of Complexes 6 and 7. The molecular structures of the electron-precise complexes 6 and 7 are shown in Figures 1 and 2; relevant band lengths and angles are summarized in Table VI.

The two independent molecules in the crystal lattice of 7 are practically identical except for the Fe1–Fe2 distance which differs very slightly but significantly with respect to the 3σ criterion (cf. Table VI). 6 and 7 are strongly related to the parent complex [Fe$_2$(CO)$_6$(μ-PBu$^t_2$)(μ-PCy$_2$)] (4). As expected, the substitution of one carbonyl group by a phosphane ligand has no severe structural consequences. The basic geometry is widely the same in all three compounds: in contrast to the butterfly geometry normally observed in bis(μ-phosphido)hexacarbonyldiiron complexes[3] the Fe$_2$P$_2$ core shows (nearly) exact planarity. The dihedral angle θ between the two Fe$_2$P planes describing the fold of the core with respect to the P···P line amounts of 175.1° (for 6), 176.4°, and 179.3° (for molecules I and II in 7, respectively) whereas the crystallographically imposed C_s symmetry of 4 implies exact planarity with $\theta = 180°$.[5] Because the phosphane ligands occupy the position of an in-plane carbonyl group in 4 both 6 and 7 have approximately C_s symmetry. Also the other dimensions of the Fe$_2$P$_2$ core in 4, 6, and 7 agree very well. When Fe–Fe bonding is neglected, the coordination spheres of the iron atoms can be interpreted as distorted tetragonal pyramids with P2 located in both apical positions and P1···P2 as a common edge. The different coordination sphere of the two iron atoms is reflected in their distances to the bridging phosphorus atoms (cf. Table VI): the Fe1–P bond lengths are about 0.05 Å shorter than those in which Fe2 is involved. Of approximately the same order of magnitude is the difference between the

Table IV. Fractional Coordinates and Equivalent Isotropic Displacement Parameters (Å²) for the Non-Hydrogen Atoms of 10·CH_2Cl_2

atom	*x/a*	*y/b*	*z/c*	U_{eq}[a]
Fe1	0.00000	−0.76364(3)	0.00000	0.0267(1)
Fe2	−0.05943(2)	−0.90357(3)	−0.09607(3)	0.0275(1)
Cl1	−0.40203(7)	−0.14791(11)	−0.52252(9)	0.1018(6)
Cl2	−0.29639(7)	−0.20572(14)	−0.40356(10)	0.1128(7)
P1	−0.03772(3)	−0.73451(5)	−0.12043(4)	0.0282(2)
P2	0.04135(3)	−0.91002(5)	−0.03212(4)	0.0313(2)
P3	−0.07919(3)	−0.69352(5)	0.04082(4)	0.0277(2)
P4	−0.15089(3)	−0.86473(5)	−0.06675(4)	0.0277(2)
O1	0.1049(1)	−0.6237(2)	0.0507(2)	0.0639(9)
O2	−0.0714(1)	−0.9607(2)	−0.2537(1)	0.0609(9)
O3	−0.0743(1)	−1.1192(2)	−0.0564(2)	0.066(1)
C1	0.0620(1)	−0.6780(2)	0.0304(2)	0.0362(9)
C2	−0.0672(1)	−0.9365(2)	−0.1914(2)	0.0377(9)
C3	−0.0684(1)	−1.0330(2)	−0.0693(2)	0.0394(10)
C4	0.0246(1)	−0.6992(2)	−0.1713(2)	0.0354(9)
C5	0.0095(2)	−0.7124(3)	−0.2576(2)	0.045(1)
C6	0.0694(2)	−0.6978(3)	−0.2867(2)	0.056(1)
C7	0.0978(2)	−0.5918(3)	−0.2659(2)	0.057(1)
C8	0.1118(2)	−0.5755(3)	−0.1811(2)	0.057(1)
C9	0.0532(2)	−0.5920(3)	−0.1502(2)	0.051(1)
C10	−0.1066(1)	−0.6498(2)	−0.1624(2)	0.0355(9)
C11	−0.0979(2)	−0.5323(2)	−0.1593(2)	0.053(1)
C12	−0.1621(2)	−0.4784(3)	−0.1780(2)	0.069(2)
C13	−0.1975(2)	−0.5068(3)	−0.2580(2)	0.065(1)
C14	−0.2036(2)	−0.6246(3)	−0.2674(2)	0.058(1)
C15	−0.1407(1)	−0.6796(3)	−0.2445(2)	0.0453(10)
C16	0.1072(1)	−0.9500(2)	−0.0800(2)	0.044(1)
C17	0.1597(2)	−0.8685(3)	−0.0630(2)	0.060(1)
C18	0.0817(2)	−0.9614(3)	−0.1655(2)	0.050(1)
C19	0.1337(2)	−1.0574(3)	−0.0519(2)	0.068(1)
C20	0.0619(2)	−0.9646(2)	0.0687(2)	0.045(1)
C21	0.0543(2)	−1.0819(3)	0.0808(2)	0.072(2)
C22	0.0155(2)	−0.9060(3)	0.1043(2)	0.050(1)
C23	0.1280(2)	−0.9288(3)	0.1116(2)	0.061(1)
C24	−0.1561(1)	−0.7492(2)	−0.0054(2)	0.0307(8)
C25	−0.0950(1)	−0.5526(2)	0.0367(1)	0.0338(8)
C26	−0.1526(2)	−0.5124(2)	0.0398(2)	0.048(1)
C27	−0.1625(2)	−0.4049(3)	0.0379(2)	0.060(1)
C28	−0.1149(2)	−0.3383(3)	0.0343(2)	0.061(1)
C29	−0.0573(2)	−0.3771(3)	0.0332(2)	0.059(1)
C30	−0.0467(1)	−0.4841(2)	0.0346(2)	0.046(1)
C31	−0.0707(1)	−0.7127(2)	0.1434(2)	0.0347(8)
C32	−0.1133(2)	−0.7611(3)	0.1774(2)	0.051(1)
C33	−0.1003(2)	−0.7732(3)	0.2554(2)	0.068(2)
C34	−0.0458(2)	−0.7355(3)	0.3004(2)	0.063(1)
C35	−0.0036(2)	−0.6845(3)	0.2676(2)	0.054(1)
C36	−0.0158(1)	−0.6734(3)	0.1896(2)	0.0438(10)
C37	−0.1820(1)	−0.9702(2)	−0.0168(1)	0.0309(8)
C38	−0.2257(2)	−1.0402(3)	−0.0559(2)	0.050(1)
C39	−0.2464(2)	−1.1223(3)	−0.0189(2)	0.059(1)
C40	−0.2252(2)	−1.1359(3)	0.0573(2)	0.049(1)
C41	−0.1816(2)	−1.0683(3)	0.0961(2)	0.051(1)
C42	−0.1595(1)	−0.9869(2)	0.0599(2)	0.0454(10)
C43	−0.2225(1)	−0.8434(2)	−0.1428(1)	0.0331(8)
C44	−0.2738(1)	−0.7868(2)	−0.1314(2)	0.0410(9)
C45	−0.3276(1)	−0.7767(3)	−0.1884(2)	0.050(1)
C46	−0.3312(1)	−0.8254(3)	−0.2578(2)	0.051(1)
C47	−0.2816(2)	−0.8840(3)	−0.2686(2)	0.051(1)
C48	−0.2271(1)	−0.8927(2)	−0.2118(2)	0.0403(9)
C49	−0.3363(3)	−0.1056(4)	−0.4572(4)	0.101(2)

[a] See footnote *a* in Table II.

Fe1–P3 bond lengths in 6 and 7 which can be explained by the different nonbridging phosphane ligands. Just as observed in 4,[5] the crystal structures of 6 and 7 show disorder phenomena: in 6 one Bu^n and one Bu^t group and in molecule I of 7 one CO ligand are disordered and could be localized in two boundary positions A and B (cf. Figures 1 and 2).

Table V. $^{31}P\{^1H\}$ NMR Data for Complexes 6–9[a,b]

	δ, ppm			*J*, Hz			
complex	P^1	P^2	P^3	P^1P^2	P^1P^3	P^2P^3	P^3H[d]
6	331.2 d (−83.3)[c]	238.8 dd (−27.6)	48.6 dd	53.3		12.6	
7	354.3 dd (−69.2)	243.6 dd (−22.8)	52.7 dd	47.7	7.1	12.5	368.2
8	295.0 dd (−0.6)	166.7 dd (−7.0)	46.0 dd	54.1	50.4	47.5	356.9
9	265.9 dt (−148.6)	196.1 dt (−70.3)	43.6 dd	79.5	8.9	14.2	

[a] P^1, μ-PBu^t_2; P^2, μ-PR_2; P^3, PR'_2R''. [b] 6, THF; 7–9, C_6H_6. [c] $\Delta\delta_{complex} - \delta_{parent}$. [d] Obtained from the ^{31}P spectra.

Table VI. Selected Bond Lengths (Å) and Angles (deg) for Compounds 6 and 7 (Molecules I and II)

	6	7 (I)	7 (II)
Fe1–Fe2	2.709(1)	2.686(2)	2.717(2)
Fe1–P1	2.229(3)	2.235(2)	2.228(2)
Fe1–P2	2.246(4)	2.220(2)	2.224(3)
Fe1–P3	2.246(2)	2.189(2)	2.197(3)
Fe1–C1	1.769(10)	1.788(8)	1.768(9)
Fe1–C2	1.768(9)	1.776(9)	1.771(9)
Fe2–P1	2.273(3)	2.275(3)	2.276(3)
Fe2–P2	2.272(3)	2.251(3)	2.257(3)
Fe2–C3	1.789(12)	1.777(11)	1.793(11)
Fe2–C4A	1.755(13)	1.774(25)	1.749(11)
Fe2–C4B		1.697(27)	
Fe2–C5	1.781(11)	1.761(11)	1.752(11)
P1–Fe1–P2	107.26(12)	107.70(9)	106.95(9)
P1–Fe2–P2	104.89(11)	105.27(9)	104.22(9)
Fe1–P1–Fe2	74.00(11)	73.10(9)	74.19(9)
Fe1–P2–Fe2	73.70(12)	73.84(9)	74.64(9)
P1–Fe1–P3	137.00(11)	146.49(8)	147.75(9)
P1–Fe1–C1	87.6(3)	85.4(3)	86.2(3)
P1–Fe1–C2	87.8(4)	88.8(3)	88.2(3)
P2–Fe1–P3	115.75(12)	105.67(9)	105.29(10)
P2–Fe1–C1	104.0(4)	107.4(3)	108.5(3)
P2–Fe1–C2	101.2(4)	101.9(3)	105.1(3)
P1–Fe2–C3	87.3(4)	89.3(4)	90.2(4)
P1–Fe2–C4A	160.4(4)	164.4(6)	163.6(3)
P1–Fe2–C4B		154.4(9)	
P1–Fe2–C5	86.9(5)	85.3(4)	86.3(4)
P2–Fe2–C3	110.6(4)	107.9(3)	107.2(3)
P2–Fe2–C4A	94.7(4)	83.4(6)	91.9(3)
P2–Fe2–C4B		98.0(9)	
P2–Fe2–C5	109.5(5)	114.4(4)	114.0(4)
Fe1–C1–O1	172.7(7)	175.0(6)	173.1(6)
Fe1–C2–O2	173.0(8)	176.8(6)	174.1(6)
Fe2–C3–O3	174.1(6)	177.4(9)	174.5(8)
Fe2–C4A–O4A	175.8(10)	175.5(14)	175.4(6)
Fe2–C4B–O4B		168.6(18)	
Fe2–C5–O5	172.5(8)	175.3(8)	173.0(8)

Reaction of $[Fe_2(CO)_5(\mu\text{-}PBu^t_2)(\mu\text{-}PCy_2)]$ (2) with dppm. The dppm ligand is known preferentially to bridge metal–metal bonds.[20,21] Complex 9 had demonstrated that two phosphorus ligands can replace the two in-plane carbonyl ligands of the parent complex 4. Because these coordination sites are opposite to each other with the FeFe axis in between, it is not realistic to expect a derivative of 4 with the dppm ligand simply adopting a bridging coordination mode. Indeed, the reaction of 2 in THF with dppm under UV irradiation proceeds according to eq 3

$$\underset{\mathbf{2}}{[Fe_2(CO)_5(\mu\text{-}PBu^t_2)(\mu\text{-}PCy_2)]} + \text{dppm} \xrightarrow[-2CO]{UV} \underset{\mathbf{10}}{[Fe_2(CO)_3(\mu\text{-}PBu^t_2)(\mu\text{-}PCy_2)(\mu\text{-dppm})]} \quad (3)$$

and affords by loss of two carbonyl ligands the unsaturated pale brown complex 10 in good yield. Complex 10 exhibits three intense terminal carbonyl bands at strikingly low wavenumbers (1912, 1878, 1853 cm^{-1}). The $^{31}P\{^1H\}$ NMR spectrum (THF) exhibits four signals according to four

---

(20) Puddephatt, R. J. *Chem. Soc. Rev.* **1983**, *12*, 99.

(21) Chaudret, B.; Delavaux, B.; Poilblanc, R. *Coord. Chem. Rev.* **1988**, *86*, 191.

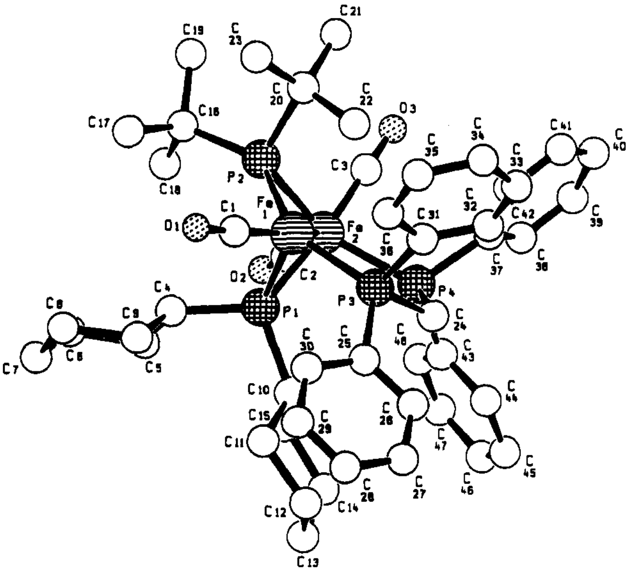

Figure 3. Molecular structure of $[Fe_2(CO)_3(\mu\text{-}PBu^t_2)(\mu\text{-}PCy_2)(\mu\text{-dppm})]$ (**10**) with atom labels.

Table VII. Selected Bond Lengths (Å) and Angles (deg) for Compound 10

Fe1–Fe2	2.631(1)	Fe2–P2	2.248(1)
Fe1–P1	2.184(1)	Fe2–P4	2.247(1)
Fe1–P2	2.223(1)	Fe1–C1	1.737(3)
Fe1–P3	2.229(1)	Fe2–C2	1.752(3)
Fe2–P1	2.288(1)	Fe2–C3	1.756(3)
P1–Fe1–P2	88.03(3)	P1–Fe2–C3	173.61(10)
P1–Fe2–P2	84.90(3)	P2–Fe2–P4	135.30(3)
Fe1–P1–Fe2	72.03(3)	P2–Fe2–C2	111.19(10)
Fe1–P2–Fe2	72.08(3)	P2–Fe2–C3	88.97(10)
P1–Fe1–P3	96.86(3)	P4–Fe2–C2	113.51(10)
P1–Fe1–C1	107.30(9)	P4–Fe2–C3	88.94(10)
P2–Fe1–P3	145.60(2)	C2–Fe2–C3	93.0(1)
P2–Fe1–C1	106.37(9)	Fe1–C1–O1	177.6(2)
P3–Fe1–C1	104.57(9)	Fe2–C2–O2	178.1(2)
P1–Fe2–P4	94.13(3)	Fe2–C3–O3	175.8(2)
P1–Fe2–C2	90.89(10)		

nonequivalent phosphorus atoms (δ 218.2 (dd, $\mu\text{-}P^1Bu^t_2$), 202.2 (dd, $\mu\text{-}P^2Cy_2$), 63.2 and 59.4 (m and dd, respectively, for the ^{31}P nuclei of the dppm ligand, designated as P^3 and P^4, with P^3 arbitrarily assigned to the unsaturated iron atom)). Spectrum simulation revealed the following coupling constants: $J(P^1P^2) = 76.0, J(P^1P^3) = 70.0, J(P^1P^4) = 65.6, J(P^2P^3) = 38.4, J(P^2P^4) = 0, J(P^3P^4) = 134.4$ Hz. The spectroscopic data did not allow a structural proposal to be made. Thus, an X-ray crystal structure determination was performed. **10** crystallizes from a solvent mixture containing dichloromethane as the solvated species $\mathbf{10}\cdot CH_2Cl_2$ which was the subject of investigation. As a result, the solvent molecules are located at holes between the complex molecules within the crystal lattice. A careful inspection of the intermolecular contact distances did not give any indication of special interactions between solvent and complex molecules and, thus, for a noticeable influence of the former on the molecular structure of the latter. Therefore, in the following only the molecular structure of **10** will be discussed. The results of the X-ray analysis confirmed the assumed structure of **10** (cf. eq 3) as a triply-bridged low coordinated 32e diiron complex with two nonequivalent metal atoms. Its molecular structure is illustrated by Figure 3; relevant geometric bonding parameters are presented in Table VII.

The synthesis of **10** from the electron-deficient complex $[Fe_2(CO)_5(\mu\text{-}PBu^t_2)(\mu\text{-}PCy_2)]$ (**2**) by replacement of two CO groups by the bidentate dppm ligand suggests the comparison of the structures of both compounds. The Fe_2P_2 core in **2** is not far from planarity (θ = 169.4°) and has a rather short Fe–Fe distance of 2.472(1) Å.[5] In contrast to this, the Fe_2P_2 core in **10** is characterized by a strongly folded butterfly geometry (θ = 107.6°) and a long Fe–Fe distance of 2.631(1) Å, clearly indicating a single bond between the iron atoms. The atom Fe1 has (ignoring the Fe–Fe bond) coordination number four and an irregular coordination geometry (cf. Table VII). The coordination sphere of Fe2 may be described by a strongly distorted trigonal bipyramid with P1 and C3 in apical positions. With respect to the distances of the iron atoms to the P and C ligator atoms the nonequivalence of Fe1 and Fe2 is in **10** less evident than in **2**. In the parent complex **2** bond lengths Fe1–P are about 0.20 Å shorter than Fe2–P whereas in **10** this difference is only 0.05 Å and the Fe1–C1 distance (1.737(3) Å) is scarcely significantly shorter than Fe2–C2 (1.752(3)) or Fe2–C3 (1.756(3) Å), respectively. The electron deficiency of Fe1 is obviously better counterbalanced by three (as in **10**) than by only two bonded phosphorus atoms (as in **2**). The five-membered Fe_2P_2C is rather unsymmetric and to a minor extent nonplanar. The two Fe–Fe–P angles differ from each other by about 10°, and the Fe–P–C angles, by about 7°. According to the observed torsion angles, the ring conformation can be described as envelope with P4 in the flap position.

The three planes defined by the two iron atoms and one or two bridging phosphorus atoms, respectively, make the following angles: Fe1,Fe2,P1/Fe1,Fe2, P2 115.8°, Fe1,Fe2,P1/Fe1,Fe2,P3,P4 92.3°, Fe1,Fe2,P2/Fe1,Fe2,P3,P4 151.9°.

The 32e complex **10** formally resembles the doubly-bridged diiron pentacarbonyl complexes **1**–**3** in that one of the iron atoms bears two, the other three, 2e ligands. The iron–iron distance in **10**, however, reveals only a single bond between the metal atoms. As shown by EHT calculations,[3] 32e complexes of the type $[Fe_2L_5(\mu\text{-}PR_2)_2]$ have to be (nearly) planar in order to form the iron–iron double bond. For complex **10** this precondition is prevented by the μ-dppm ligand. The formation of complex **10** thus (i) nicely underlines the reality of the iron–iron double bond in complexes **1**–**3** and its importance for their structure, (ii) shows the dominance of the tendency of the dppm ligand to bridge metal–metal bonds over that of the $Fe(\mu\text{-}PBu^t_2)(\mu\text{-}PCy_2)Fe$ core to remain planar, and (iii) reveals a (previously unexpected) flexibility of this sterically crowed core. These conclusions suggest that molecules such as **2** and **3**, but also **10** itself, are well suited for a wide range of chemistry.

While this paper was being finished, Hogarth and Lavender[22] described the closely related but saturated complexes $[Fe_2(CO)_4(\mu\text{-}PPh_2)(\mu\text{-}PR_2)(\mu\text{-dppm})]$ (R = Ph, Cy). These compounds confirm the importance of the bulkiness of the phosphido bridges to induce the low coordination in complex **10**.

Acknowledgment. The authors are grateful to the Fonds der Chemischen Industrie for support.

OM930148+

---

[22] Hogarth, G.; Lavender, M. H. *J. Chem. Soc., Dalton Trans.* **1993**, 143.